Crystal Structures of 1,3-Distearoyl-2-oleoylglycerol and Cocoa Butter in the β(V) Phase Reveal the Driving Force Behind the Occurrence of Fat Bloom on Chocolate

René Peschar,* Mihaela M. Pop, Dirk J. A. De Ridder, Jan B. van Mechelen, René A. J. Driessen, and Henk Schenk

Laboratory for Crystallography, van't Hoff Institute for Molecular Sciences, Faculty of Science, Universiteit van Amsterdam, Nieuwe Achtergracht 166, NL-1018 WV Amsterdam, The Netherlands

Received: July 23, 2004; In Final Form: August 26, 2004

On the basis of high-resolution synchrotron powder diffraction data, crystal structures have been solved for 1,3-distearoyl-2-oleoylglycerol, a major *cis*-mono-unsaturated triglyceride fraction of cocoa butter, and cocoa butter itself in the β(V) phase. The latter implies that in fact a crystal structure model of chocolate in the β(V) phase has been obtained. The results clarify the metastability of the β(V) phase and explain why fat bloom may develop on β(V)-type chocolate that has been stored at temperatures that are too high.

Introduction

cis-Mono-unsaturated triglycerides (TAGs) are the main constituents of natural oils and fats, and their polymorphism determines the quality of food products and confectionaries to a large extent. An example is chocolate that consists of a cocoa butter (CB) matrix in which fine cocoa powder and sugar particles are dispersed. Greatly appreciated properties of chocolate, such as its gloss, the "snap" when it breaks, and its fast complete melting at body temperature that provides a cooling effect in the mouth are mainly determined by the crystalline form and melting behavior of the CB phase that mainly consists of *cis*-mono-unsaturated TAGs.[1] Out of the six crystalline forms known for CB[2], in good-quality chocolate CB should be crystallized in one of its two highest melting forms, the β(V) form[2] or the β(VI) form.[3] Chocolate that has been stored too long at temperatures that are too high may develop fat bloom, an unattractive whitish layer. Fat bloom development has commonly been attributed to the phase transition β(V) → β(VI) of the cocoa butter.[4−6] Although various theories have been set up to explain this phase transition (e.g. phase separation[6,7] and solid-state polymorphic transformation[2,7]), the precise mechanism is still not known, one reason being that crystal structure models of *cis*-mono-unsaturated TAGs are not available.

The *cis*-mono-unsaturated TAG 1,3-distearoyl-2-oleoylglycerol (SOS) plays a major role in the crystallization of CB into its β forms[8,9] and possibly also in the transition of β(V) to β(VI). Powder diffraction patterns of the β_2 phase of SOS (the highest but one melting β phase of SOS,[10] abbreviated hereafter as β-SOS), the β(V) phase of CB,[11] and the pattern of β(V) chocolate, from which the sugar has been removed by washing it out with cold water, are all strikingly similar (Figure 1). Structure determination from powder data has been successful for mono-acid-saturated TAGs[12−14] using direct-space search techniques that rely on the overall homology of a series of TAGs and the availability of a single-crystal-based model.[15] For β-SOS, no such model analogue was available, and we had to resort to a new generation of more versatile direct-space search techniques to obtain its crystal structure. Very surprisingly, starting from the crystal structure of β-SOS a crystal structure model of CB in the β(V) phase could also be obtained.

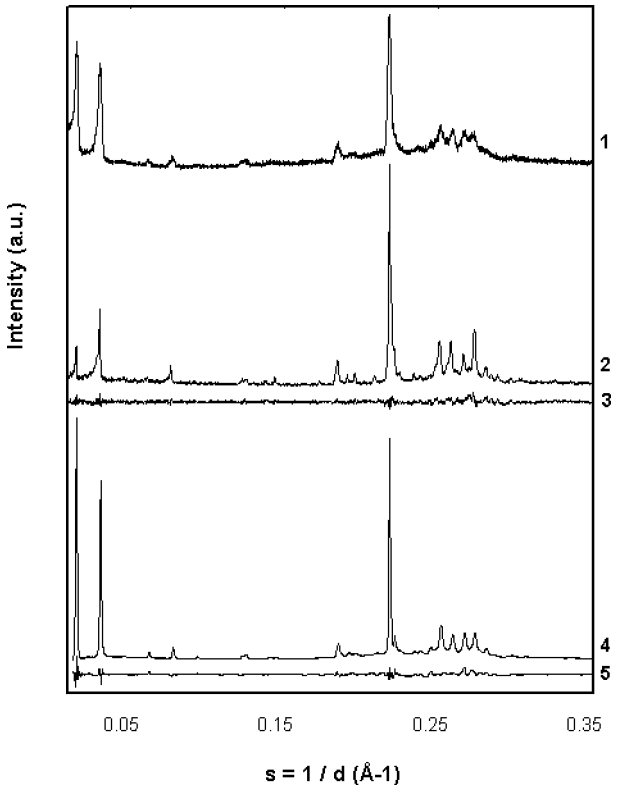

Figure 1. Experimental powder diffraction data of chocolate and its constituents. Laboratory X-ray powder diffraction pattern of β-V chocolate (sugar washed out) (pattern 1). Synchrotron powder diffraction pattern and the difference pattern after the final Rietveld refinement of SOS (λ = 0.4093 Å, patterns 2 and 3). Synchrotron powder diffraction pattern and the difference pattern after the final Rietveld refinement of β-V Ivory Coast cocoa butter (λ = 0.79998 Å, patterns 4 and 5). For comparison, all patterns are shown as function of $s = 1/d$ (in Å^{-1}).

Materials and Methods

Sample Preparation and Data Collection. Samples of SOS and CB from the Ivory Coast were established to be in

* Corresponding author. E-mail: rene@science.uva.nl.

10.1021/jp046723c CCC: $27.50
Published on Web 09/14/2004

the β(V) polymorph by laboratory X-ray powder diffraction. For this purpose, first the CB was molten completely and stored at room temperature (~22 °C) for several weeks. High-resolution synchrotron powder diffraction data of the SOS and CB samples were collected at beamlines BM16 (T = 273 K) and BM01B (Swiss−Norwegian CRG; T = 293 K) of the European Synchrotron Radiation Facility (Grenoble, France), respectively, in a continuous scanning mode and finally binned at a step size of 0.005 °2θ.

Crystal Structure Determination and Refinement. Auto-indexing techniques were not successful in determining the unit cells, probably because of the extreme length differences of the unit cell axes. Unit cells have been obtained with an indexing routine written especially for this purpose and implemented in POWSIM,[16] in which trial unit-cell parameters can be changed systematically in user-defined intervals.

A starting model of SOS was created by substitution of the 2-stearoyl chain of the β-SSS model[13] by an oleoyl chain.[17] Structure determination of SOS was carried out with the help of the programs FOX[18] and ORGANA,[19] the refinement using soft constraints with the Rietveld module in the GSAS package.[20]

Nearly three-quarters of any CB consists of SOS and two other *cis*-mono-unsaturated TAGs, 2-oleoyl-1-palmitoyl-3-stearoylglycerol (POS) and 1,3-dipalmitoyl-2-oleoylglycerol (POP).[21] Compared with SOS, molecules of POS and POP have one and two fewer $-CH_2CH_2-$ groups in the saturated chains, respectively, and in view of the similarity of the diffraction patterns of β-SOS and β(V)-CB (cf. patterns 2 and 4 in Figure 1), it was assumed that in CB all three TAGs are cocrystallized in the same lattice. Therefore, the CB model was taken as β-SOS with a partial occupancy (57%) of the two end-carbon atoms of the S_1 and S_3 chains, as calculated from a simplified average CB TAG composition of 35% POS, 23% SOS, and 13% POP. Refinement using soft constraints was again carried out with the Rietveld module in the GSAS package.[20]

Details of the indexing procedure, structure determination, and Rietveld refinement will be communicated elsewhere.

Geometric Analysis. To analyze the structures of β-SOS and β(V)-CB, two geometrical parameters are useful: the chain direction, which is the least-squares line through a set of atoms, and the chain plane, which is the least-squares plane through a set of atoms. Four (partial) chains are considered: the S_1 and S_3 chains consisting of all of their C sp^3 atoms and the two parts of the O chain that are linked by the double bond, the O(C_1-C_9) and the O($C_{10}-C_{18}$) chains (Figure 2).

Results and Discussion

Crystallographic data for SOS and β(V)-CB are summarized in Table 1. The final structural models of SOS and β(V)-CB obtained after the Rietveld refinement using soft constraints by means of the GSAS package produced a good fit to the respective diffraction patterns (Figure 1, patterns 2 and 3 for SOS, patterns 4 and 5 for β(V)-CB), and the calculated density for SOS (Table 1) agrees well with experimental data known from the literature.[22] For β(V)-CB, the refined occupancy factors of the end carbon atoms of both S chains differed less than 2% from their starting values. The χ^2 of the β(V)-CB is much higher than that of SOS because the minimization function in GSAS includes the weighted differences related to the imposed restraints, and these were released less in β(V)-CB than in SOS.

The overall stacking of the molecules in β-SOS and β(V)-CB is similar. Both are crystallized in a 1,3 tuning-fork conformation with a triple chain-length packing (Figure 3) that consists of alternating layers of saturated S and unsaturated O chains with the S_1 chain being extended somewhat relative to the S_3 chain (Figure 2). Corresponding chain directions in β-SOS and β(V)-CB differ less than 10°, and the S_1, S_3, and O($C_{10}-C_{18}$) chain directions are almost parallel (interchain angles <8°). The O(C_1-C_9) chain direction, however, is not parallel to the other three chain directions, with interchain angles ranging from 42 to 46° in β-SOS and 32−39° in β(V)-CB. This

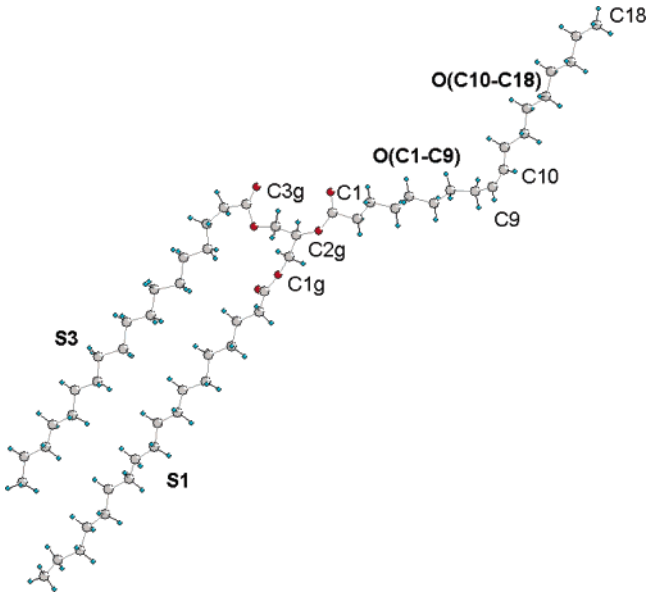

Figure 2. Molecular structure of 1,3-distearoyl-2-oleoylglycerol (SOS) and atomic numbering of relevant atoms.

TABLE 1: Experimental Details for 1,3-Distearoyl-2-oleoylglycerol (SOS) in the β_2 Phase and Ivory Coast Cocoa Butter in the β(V) Phase

	SOS β_2 phase	Ivory Coast cocoa butter β(V) phase
	crystal data	
chemical formula	$C_{57}H_{108}O_6$	$C_{55.28}H_{103.69}O_6$
chemical formula weight	889.48	866.5
space group	$P\bar{1}$ (no. 2)	$P\bar{1}$ (no. 2)
a (Å)	8.211(3)	8.225(3)
b (Å)	65.357(18)	64.18(2)
c (Å)	5.4624(6)	5.4451(6)
α (deg)	87.78(2)	87.52(2)
β (deg)	88.83(2)	88.73(2)
γ (deg)	89.72(4)	89.84(4)
V (Å^3)	2928.7(14)	2870.7(14)
Z	2	2
wavelength (Å)	0.4093	0.79998
D_x (Mg m^{-3})	1.009	1.000
temperature (K)	273	293
	Data Collection and Refinenent	
diffractometer	BM16 (ESRF)	BM01B (ESRF)
2θ region (deg)	0.165−14.995	0.605−30.0
no. of data points	2967	5880
no. of variables	189	191
no. of soft constraints	178	180
R_p (%)[a,d]	9.1	6.9
	8.0	6.6
R_{wp} (%)[b,d]	11.8	9.6
	9.5	9.4
$\chi^{2\,c,d}$	4.6	14.8
	3.6	12.9

[a] $R_p = \Sigma|y_{obsd} - y_{calcd}|/\Sigma\, y_{obsd}$. [b] $R_{wp} = \{\Sigma\, w(y_{obsd} - y_{calcd})^2/\Sigma\, wy_{obsd}^2\}^{1/2}$. [c] $\chi^2 = \{\Sigma\, w(y_{obsd} - y_{calcd})^2/N - P\}^{1/2}$, N = number of observations, P = number of variables [d] R_p, R_{wp}, and χ^2 list the results of the GSAS refinement. Each second line lists the value calculated with the background being subtracted.

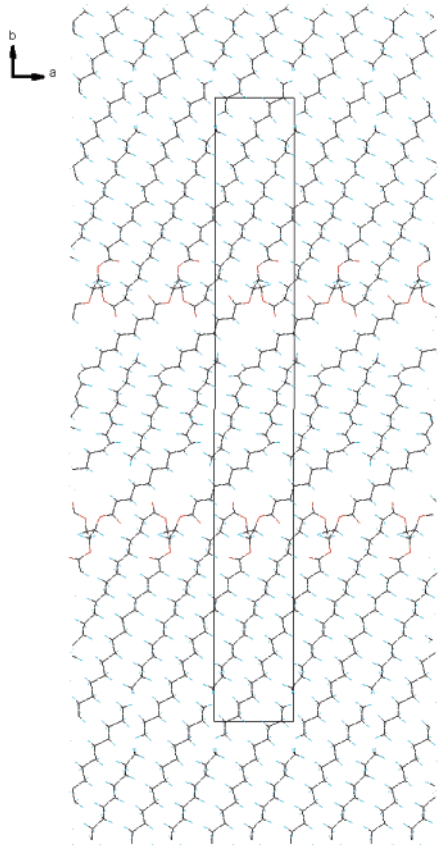

Figure 3. Crystal structure of β-V Ivory Coast cocoa butter. Packing diagram viewed along the *c* axis.

differs clearly from postulated SOS models[10,23,24] in which O(C_1−C_9) is depicted as being parallel to S_1 and S_3.

The postulated β-SOS models[10,23,24] also have a close-packed oleoyl layer with $\pi-\pi$ interactions at the C_9═C_{10} double bond. However, in the crystal structures of β-SOS and β(V)-CB, a considerably different packing is found. Within the oleoyl layer, the O(C_{10}−C_{18}) of neighboring O chains and the C_9═C_{10} are related via a center of symmetry (Figure 3), but interactions between the O(C_1−C_9) and O(C_{10}−C_{18}) of neighboring O chains as well as double bond $\pi-\pi$ interactions are absent. The absence of the latter combined with weaker van der Waals interactions in the O chains implies an enhanced structural flexibility and may explain why higher-melting β polymorphs exist (β(VI)-CB and the highest-melting (β_1) polymorph of SOS[10]). It seems likely that these latter polymorphs will show stronger interactions in the O-chain region.

In absence of unit-cell parameters, TAGs are often characterized in terms of their subcell packing.[25] Apart from powder diffraction, various other techniques have been used for this purpose, especially Fourier transform infrared (FT-IR)[26,27] and cross-polarization magic-angle nuclear magnetic resonance.[28] With respect to β-SOS, for the stearoyl leaflet a triclinic subcell ($T_{||}$) [25] has been proposed.[26] In contrast to trisaturated monoacid β-TAGs,[12−15] the concept of a common triclinic subcell is not applicable to the full crystal structures of β-SOS and β(V)-CB because of the S_1−S_3 interchain plane angle (∼30°) (Figure 4). The tilt angle of the acyl chains toward the lamellar interfaces is determined by the tilt angle between the *a* axis and the S_1 and S_3 chain directions and ranges in β-SOS and β(V)-CB from 63 to 66°, almost equal to the angle (67°) calculated for triple-chain-packed β-saturated TAG systems with an underlying $T_{||}$ subcell[24] but appreciably higher than values

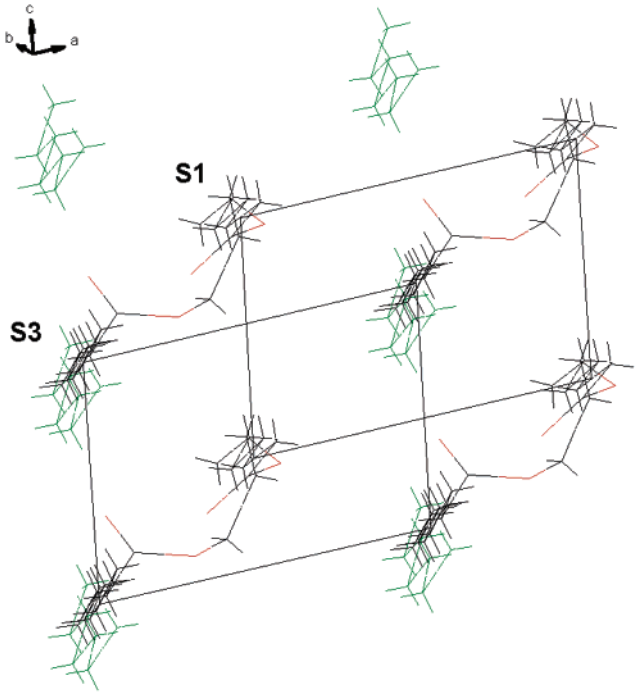

Figure 4. Crystal structure of β-V Ivory Coast cocoa butter. $T_{||}$ subcell packing of the S chains and the C_{10}−C_{18} part of the oleoyl chain in gray and green, respectively, viewed along the chains.

(52−54°) that were derived for β-SOS from X-ray powder data.[10,24] The absence of a common subcell corroborates with FT-IR results that indicated differences in the subcell packing of the S and O chains in β-SOS.[26,27]

Torsion angle conformations of the *cis*-oleic fragment C_8−C_9═C_{10}−C_{11} in β-SOS and β(V)-CB are different (−106, 5, −174° and −173, 0, 179°, respectively). They also differ from the conformation in the oleic acid model[17] used (120, 0, −120°) to solve the structure of SOS and from the conformations in the β phase of oleic acid (173.9, −0.7, 173.0° and 174.9, −0.6, 174.9°)[29] and the conformation in the most commonly referred to model of β-SOS.[11] Because the glycerol conformations in β-SOS, β(V)-CB, and the mono-acid β-TAGs[12−15] also show large variations in dihedral angles, it is concluded that the torsion angle conformations of these moieties are not indicative of the final TAG packing. In this respect, the similarity of chain directions and the S_1−S_3 interchain plane angle appear to be more important parameters.

Our findings clarify the driving force behind the slow transition from the metastable β(V) to the stable β(VI) polymorph. The packing of SOS, POS, and POP in β(V)-CB has a β-SOS-like structure in which on average only 57% of the two carbon positions at the end of the saturated chains are occupied and 43% are ethyl-end "holes". The absence of interactions at these holes causes β (V)-CB to be metastable and is likely to be the driving force for the transformation to the β(VI) form, implying a structural reorganization that reduces the number of directly opposing holes. It can be envisaged that this process may take place either via a solid-state β(V) to β(VI) transformation or via a melt-mediated process in which the β(V) dissolves in the melt and β(VI) crystallizes.[30] In either case, the resulting β(VI)-type packing will be dominated by β-POS, with SOS and POP being cocrystallized, in a $T_{||}$ subcell packing of the chains, as suggested by FT-IR results.[27] Additional experimental evidence for this is the striking similarity between powder patterns of β-POS and β(VI)-CB (Figure S1). To our knowledge,

this similarity has gone unnoticed so far and is far better than the mentioned resemblance[31] between powder patterns of β_1-SOS and β(VI)-CB as illustrated in Figure S1 (Supporting Information).

Acknowledgment. We thank Unilever Research NL and ADM Cocoa NL for providing the samples of SOS and Ivory Coast cocoa butter, respectively. We thank H. Emerich, W. van Beek (both ESRF, BM01B) and E. Doryhee (ESRF, BM16) for support at the ESRF. From the staff of the Laboratory for Crystallography (UvA,NL), we thank A. van Langevelde, R.B. Helmholdt, K. Goubitz, and W. Molleman for help with the synchrotron data collection and V. Brodski for help with the structure determination. Support from The Netherlands Technology Foundation (STW) of The Netherlands Foundation for Chemical Research (NWO/CW), (grants 790.35.5404 and 790.35.5616) is acknowledged, as well as support from Loders Croklaan NL, Unilever Colworth UK, ADM Cocoa NL, Gerkens Cacao NL, Koninklijke De Ruyter NL, Barry Callebaut B, and Nestlé NL. We thank members of the STW user committees 790.35.5404 and 790.35.5616 for stimulating discussions.

Supporting Information Available: Fingerprint area of high-resolution synchrotron powder diffraction patterns as functions of $s = 1/d$ (in Å^{-1}). This material is available free of charge via the Internet at http://pubs.acs.org.

References and Notes

(1) *Industrial Chocolate Manufacture and Use*; Beckett, S. T., Ed.; Blackwell Science: Oxford, England, 1999.
(2) Wille, R. L.; Lutton, E. S. *J. Am. Oil Chem. Soc.* **1966**, *43*, 419.
(3) Van Malssen, K. F.; Peschar, R.; Schenk, H.; Van Langevelde, A. J. Patent WO 01/06863, 2001.
(4) Cebula, D. J.; Ziegleder, G. *Fat Sci. Technol.* **1993,** *95*, 340.
(5) Timms, R. E. *Prog. Lipid Res.* **1984**, *23*, 1.
(6) Schlichter-Aronhime, J.; Garti, N. In *Crystallization and Polymorphism of Fats and Fatty Acids*; Garti, N., Sato, K., Eds.; Marcel Dekker: New York, 1988; Chapter 9.
(7) Bricknell, J.; Hartel, R. W. *J. Am. Oil Chem. Soc.* **1998**, *75*, 1609.
(8) Van Langevelde, A.; Van Malssen, K.; Peschar, R.; Schenk, H. *J. Am. Oil Chem. Soc.* **2001**, *78*, 919.
(9) Van Langevelde, A.; Driessen, R.; Molleman, W.; Peschar, R.; Schenk, H. *J. Am. Oil Chem. Soc.* **2001**, *78*, 911.
(10) Sato, K.; Arishima, T.; Wang, Z. H.; Ojima, K.; Sagi, N.; Mori, H. *J. Am. Oil Chem. Soc.* **1989**, *66*, 664.
(11) Sato, K.; Ueno, S. In *Crystallization Processes in Fats and Lipid Systems*; Garti, N., Sato, K., Eds.; Marcel Dekker: New York, 2001; Chapter 5.
(12) Van Langevelde, A. J.; Peschar, R.; Schenk, H. *Acta Crystallogr., B* **2001**, *57*, 372.
(13) Van Langevelde, A. J.; Peschar, R.; Schenk, H. *Chem. Mater.* **2002**, *13*, 1089.
(14) Helmholdt, R. B.; Peschar, R.; Schenk, H. *Acta Crystallogr., B* **2002**, *58*, 134.
(15) Van Langevelde, A.; Van Malssen, K.; Hollander, F.; Peschar, R.; Schenk, H. *Acta Crystallogr., B* **1999**, *55*, 114.
(16) Peschar, R.; Etz, A.; Jansen, J.; Schenk, H.; In *Structure Determination from Powder Diffraction Data*; David, W. I. F., Shankland, K., McCusker, L. B., Baerlocher, Ch., Eds.; Oxford University Press: Oxford, England, 2002; Chapter 10.
(17) Abrahamsson, S.; Ryderstedt-Nahringbauer, I. *Acta Crystallogr.* **1962**, *15*, 1261.
(18) Favre-Nicolin, V.; Černý, R. *J. Appl. Crystallogr.* **2002**, *35*, 734.
(19) Brodski, V.; Peschar, R.; Schenk, H. *J. Appl. Crystallogr.* **2003**, *36*, 239.
(20) Larson, A. C.; Von Dreele, R. B. *GSAS, General Structure Analysis System*; Report No. LA-UR-86-748 Los Alamos National Laboratory: 1987.
(21) Sato, K.; Ueno, S.; Yano, J. *Prog. Lipid Res.* **1999**, *38*, 91.
(22) Arishima, T.; Sagi, N.; Mori, H.; Sato, K. *J. Jpn. Oil Chem. Soc.* **1995**, *44*, 431.
(23) Larsson, K. *Fette, Seifen, Anstrichm.* **1972**, *74*, 136.
(24) De Jong, S.; Van Soest, T. C.; Van Schaick, M. A. *J. Am. Oil Chem. Soc.* **1989**, *68*, 371.
(25) Hernqvist, L. In *Crystallization and Polymorphism of Fats and Fatty Acids*; Garti, N., Sato, K., Eds.; Marcel Dekker: New York, 1988; Chapter 3.
(26) Yano, J.; Ueno, S.; Sato, K.; Arishima, T.; Sagi, N.; Fumitoshi, K.; Kobayashi, M. *J. Phys. Chem.* **1993**, *97*, 12967.
(27) Yano, J.; Sato, K.; Kaneko, F.; Small, D. M.; Kodali, D. R. *J. Lipid Res.* **1999**, *40*, 140.
(28) Arishima, T.; Sugimoto, K.; Kiwata, R.; Mori, H.; Sato, K. *J. Am. Oil Chem. Soc.* **1996**, *73*, 1231.
(29) Kaneko, F.; Yamazaki, K.; Kitagawa, K.; Kikyo, T.; Kobayashi, M.; Kitagawa, Y.; Matsuura, Y.; Sato, K.; Suzuki, M. *J. Phys. Chem. B* **1997**, *101*, 1803.
(30) Sato, K.; Koyano, T. In *Crystallization Processes in Fats and Lipid Systems*; Garti, N.; Sato, K., Eds.; Marcel Dekker: New York, 2001; Chapter 12.
(31) Sato, K. In *Advances in Applied Lipid Research*; Padley, F., Ed.; JAI Press: London, 1996; pp 213−268.